nature climate change

ARTICLES

https://doi.org/10.1038/s41558-022-01437-y

A climate risk index for marine life

Daniel G. Boyce[1,2]✉, Derek P. Tittensor[1,3], Cristina Garilao[4], Stephanie Henson[5], Kristin Kaschner[6], Kathleen Kesner-Reyes[7], Alex Pigot[8], Rodolfo B. Reyes Jr.[7], Gabriel Reygondeau[9], Kathryn E. Schleit[10], Nancy L. Shackell[2], Patricia Sorongon-Yap[7] and Boris Worm[1]

Climate change is impacting virtually all marine life. Adaptation strategies will require a robust understanding of the risks to species and ecosystems and how those propagate to human societies. We develop a unified and spatially explicit index to comprehensively evaluate the climate risks to marine life. Under high emissions (SSP5-8.5), almost 90% of ~25,000 species are at high or critical risk, with species at risk across 85% of their native distributions. One tenth of the ocean contains ecosystems where the aggregated climate risk, endemism and extinction threat of their constituent species are high. Climate change poses the greatest risk for exploited species in low-income countries with a high dependence on fisheries. Mitigating emissions (SSP1-2.6) reduces the risk for virtually all species (98.2%), enhances ecosystem stability and disproportionately benefits food-insecure populations in low-income countries. Our climate risk assessment can help prioritize vulnerable species and ecosystems for climate-adapted marine conservation and fisheries management efforts.

Climate change is a pervasive driver of ecological change and biodiversity loss[1,2], with adverse consequences for ecosystem health[3,4], food security[5–7] and human well-being[8]. Climate-smart management and conservation strategies are needed to ensure the effective stewardship of living resources now and in the future[9–11]. The success of these strategies requires a robust understanding of the differential vulnerability of species and ecosystems to climate change[11–13]. While climate change vulnerability assessments (CCVAs) have been advocated as an essential strategy[11–13], existing frameworks have not found broad application in conservation and management contexts.

One key factor inhibiting the broader application of CCVAs has been the challenge of evaluating species vulnerability comprehensively across three fundamental dimensions: (1) their encounter with hazardous climate conditions (exposure), (2) their susceptibility (sensitivity) and (3) their resilience to those conditions (adaptivity)[14–17]. To date, most CCVAs have analysed only one or two of these dimensions[16], providing an incomplete picture. Moreover, many CCVAs are not spatially explicit but calculate a single vulnerability score across the species' distributional range (exceptions include refs. [18–20]), potentially obscuring spatial variation that is critical to management and conservation objectives. CCVAs often incorporate expert opinions rather than quantitative empirical data[12,17,19], limiting their reproducibility and ability to track changing vulnerability through time. Finally, vulnerability is almost exclusively reported in dimensionless units to compare and rank species' relative vulnerabilities[12,15–20], limiting their application because stakeholders often require explicit risk assessments on an absolute scale. New approaches that augment existing CCVAs to address this suite of limitations are thus needed to broaden their application; simplify communication among scientists, conservation managers and stakeholders; and facilitate climate-smart management strategies[9,11,12].

We address these limitations and develop an empirically rooted, spatially explicit framework to assess both relative climate vulnerability and absolute climate risk for all available marine life forms, and we explore the application of this framework to conservation planning and socio-economic development. We evaluate climate risk for 24,975 marine species and ecosystems globally under two contrasting greenhouse gas emission scenarios (SSP5-8.5 (high emissions) and SSP1-2.6 (high mitigation)). We conclude by exploring the applied advantages of this framework for conservation and management by evaluating aggregate ecosystem climate risk in relation to priority conservation areas and assessing climate risk for exploited species within the exclusive economic zones (EEZs) of maritime countries and the high seas beyond national jurisdiction.

A climate index for marine life

Our analysis focuses on species that inhabit the upper 100 m of the water column, where climate-driven temperature changes are the most severe. The assessed marine species were primarily animals ($n = 24{,}617$ species; 98.6%) but also included plants ($n = 230$; 0.9%), chromists ($n = 72$; 0.3%), protozoans ($n = 48$; 0.2%) and bacteria ($n = 8$; <0.1%) (Extended Data Fig. 1a).

In each 1° × 1° grid cell (~111 km × 111 km at the equator) across each species' native geographic distribution[21] (Fig. 1a), validated high-resolution data sources (Supplementary Table 2) are used to calculate 12 climate indices (Fig. 1b and Supplementary Table 1). The indices comprehensively capture unique information about ecological responses to climate change and include, for instance, species' proximity to current[22] and projected future[23] hazardous climate conditions, intrinsic resilience to perturbations[24], responses to synergistic impacts[3] and climate-driven ecosystem disruption[1]. The indices are then used to calculate species' climate vulnerability and risk according to three dimensions: the present-day sensitivity to

[1]Department of Biology, Dalhousie University, Halifax, Nova Scotia, Canada. [2]Bedford Institute of Oceanography, Fisheries and Oceans Canada, Dartmouth, Nova Scotia, Canada. [3]United Nations Environment Programme World Conservation Monitoring Centre, Cambridge, UK. [4]GEOMAR Helmholtz Centre for Ocean Research, Kiel, Germany. [5]National Oceanography Centre, Southampton, UK. [6]Department of Biometry and Environmental System Analysis, University of Freiburg, Freiburg, Germany. [7]Quantitative Aquatics, Los Banos, Philippines. [8]Centre for Biodiversity and Environment Research, Department of Genetics, Evolution and Environment, University College London, London, UK. [9]Institute for the Oceans and Fisheries, Changing Ocean Research Unit, University of British Columbia, Vancouver, British Columbia, Canada. [10]Oceans North, Halifax, Nova Scotia, Canada. ✉e-mail: dboyce@dal.ca

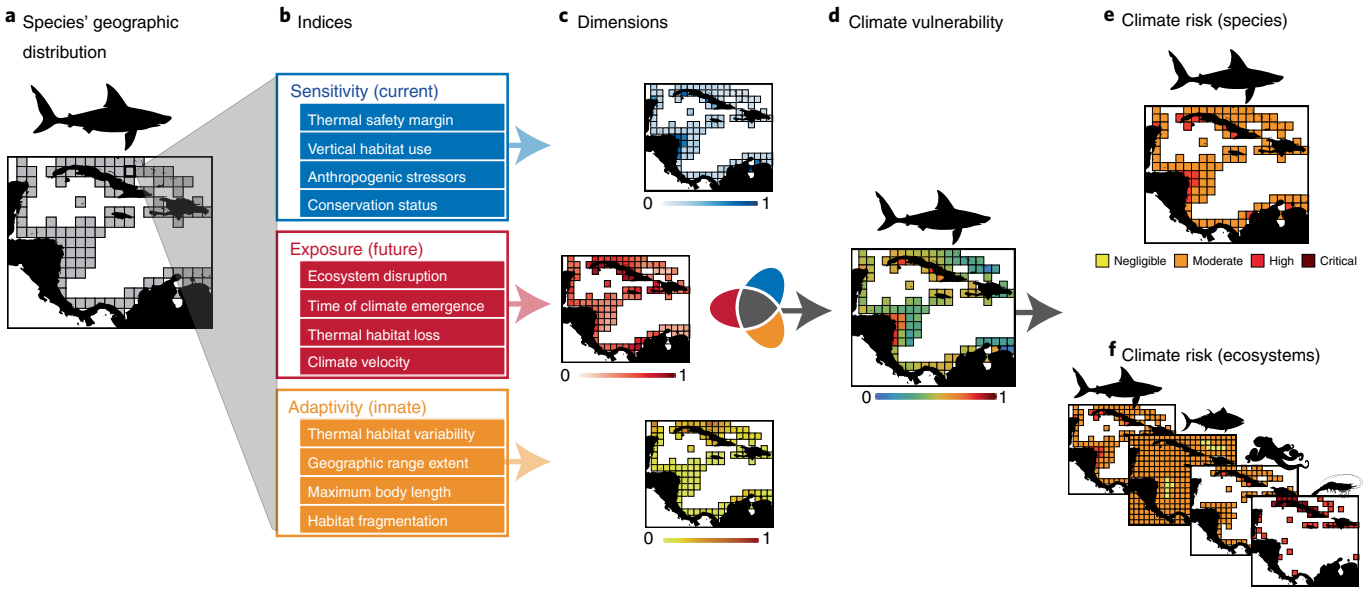

Fig. 1 | Spatially explicit assessment of climate vulnerability and risk for species and ecosystems globally. a–e, Within each grid cell (1° × 1° here) across the native geographic distribution of a species (**a**), 12 standardized climate indices are calculated (**b**) and used to define the three dimensions of climate vulnerability (**c**): present-day sensitivity (blue), projected future exposure (red) and innate adaptivity (yellow). The dimensions are used to calculate the species' climate vulnerability (**d**), and the relative vulnerability scores are translated into absolute climate risk categories (**e**). **f**, Species maps are superimposed to assess the climate vulnerability and risk for marine ecosystems. Basemaps in **a**,**c–e** from Natural Earth.

climate change, projected future exposure and innate potential to adapt (Fig. 1c). Climate vulnerability is evaluated on a relative scale from 0 to 1, with vulnerability = 1 typically corresponding to a species and location where sensitivity and exposure indices are at their extreme highest and adaptivity is at its lowest (Fig. 1d). Climate vulnerability scores are converted to an absolute risk scale ranging from negligible (lowest) to critical (highest) (Fig. 1e) using ecological thresholds (Supplementary Table 4). This absolute risk score captures both the likelihood and the magnitude of adverse consequences[25] for species at the individual locations across their distributions and the aggregate ecosystems they compose. This translation of relative vulnerability into absolute risk using thresholds is analogous to the IPCC reasons for concern framework that assesses climate risk to humans[14,26] and the widely adopted International Union for the Conservation of Nature (IUCN) Red List Index of extinction risk for species[27]. However, whereas the Red List Index assesses extinction risk at the species level and is identical across species' distributions, the climate risk index for biodiversity (CRIB) presented here disaggregates climate risk and its spatial variation across the sites throughout a species' distribution and evaluates risk for both individual species and aggregate ecosystems (Fig. 1f). Because the CRIB does not consider range expansions to new locations, it assesses the climate risk to the in situ persistence of species and the biotic intactness of their ecosystems; it represents a baseline that can be flexibly updated when confronted with new data and knowledge. See the Supplementary Information, 'Calculation of the indices', for the full methodology and an example; Extended Data Fig. 2 depicts the workflow.

Climate vulnerability of marine species

Climate vulnerability varies widely, both spatially and across species. The highest vulnerability score found in our analysis (0.92) is for a large, long-lived, range-restricted species that is heavily exploited and of critical conservation concern: Chinese puffer (*Takifugu chinensis*), at a highly impacted nearshore site near China under the high-emission scenario. The lowest vulnerability score (0.07) is for a shorter-lived, vertically migrating, mesopelagic, pan-global species, the bluntsnout lanternfish (*Myctophum obtusirostre*), at an offshore site under the low-emission scenario. Across an entire species' distribution, a range-restricted species of critical conservation concern, the Galapagos damselfish (*Asurina eupalama*), has the highest vulnerability (0.75; Fig. 2a), and the jewel fire squid, *Pterygioteuthis gemmate*, has the lowest (0.17). Substantial differences in vulnerability are seen between higher taxa (Fig. 2b).

Climate risk for marine species

The emission scenario affects species' risk by modifying their anticipated exposure to hazardous climate change. When vulnerability scores are spatially aggregated across each species' range under the high-emission scenario, 2.7% of the assessed species are at critical risk, 84% are high, 13% are moderate and virtually none (<1%) are at negligible risk (Fig. 2a) by the year 2100. In contrast, 1.3% of the assessed species under the low-emission scenario are at critical risk, 54% are high, 44% are moderate and 0.3% are at negligible risk by 2100. The benefits of emission mitigation are near-universal, with 98.2% of species less vulnerable and all species less exposed to hazardous climates (Supplementary Figs. 53 and 54). The few species that become more vulnerable under emission mitigation tend to be broadly distributed but have highly fragmented and restricted distributions (≤2% of the global area).

Despite the ubiquitous benefits of emission reduction, relative gains differ among taxa (Fig. 2b). Among animals, molluscs, ray-finned fishes (Actinopterygii) and cephalopods benefit the most from mitigation. Numerous species within these groups are targeted by fisheries, suggesting that fisheries may benefit inordinately from mitigation, as also suggested by marine ecosystem models[8]. Irrespective of emissions, 27% of species are classified as high or critical risk in their sensitivity and 47% in their adaptivity to climate impacts (Fig. 2c). In contrast, under low emissions, a minority of species (27%) are classified as highly or critically at risk of exposure to projected climate impacts, whereas under high emissions, the vast majority (98%) are at high or critical exposure risk (Fig. 2c).

While variation in climate vulnerability is the greatest among species (taxonomic coefficient of variation, 16%), there is also

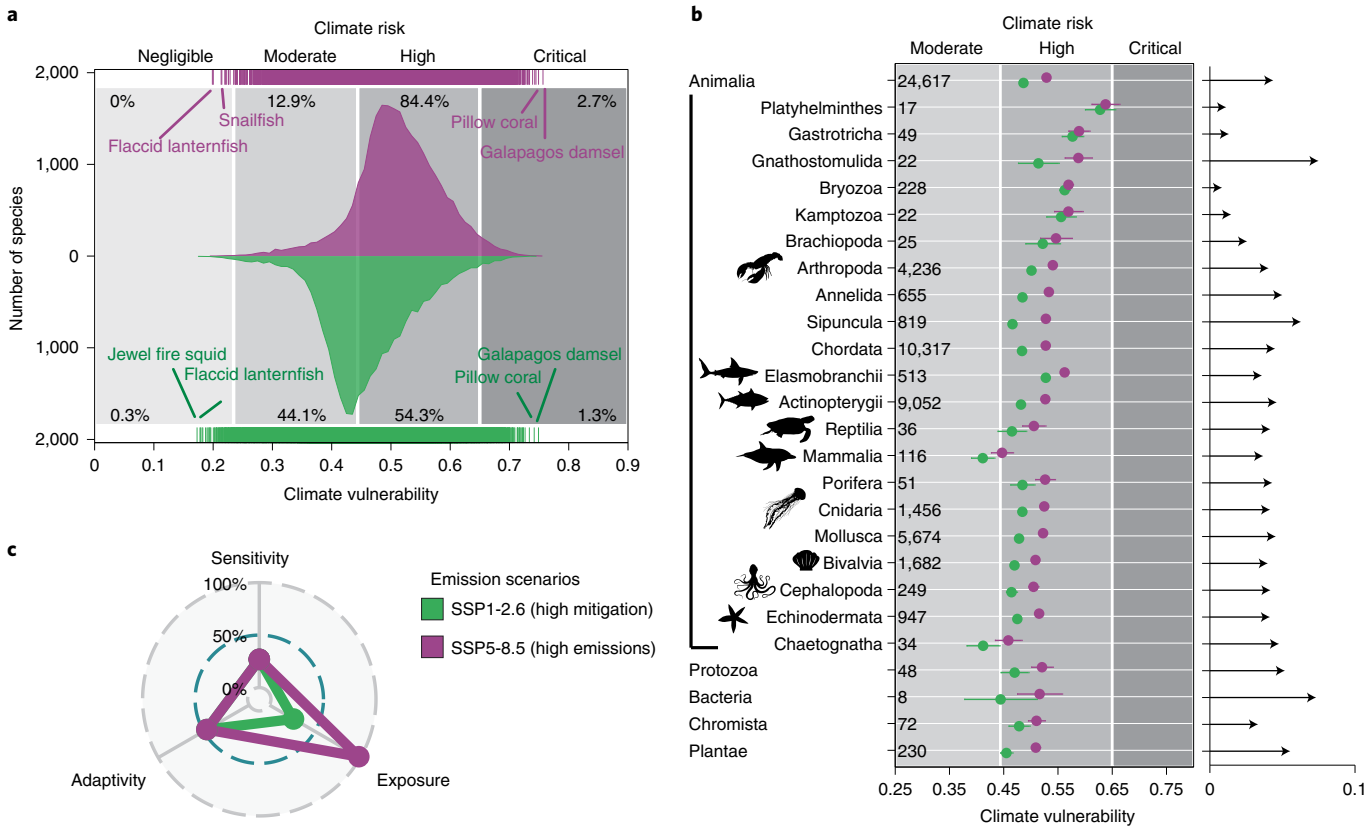

Fig. 2 | Climate vulnerability and risk for species. a, The shading depicts the numerical densities of the species vulnerability scores under contrasting emission scenarios to the year 2100. The ticks in the margins indicate the scores. The grey shading represents climate risk categories, and the colours represent the emission scenario (green indicates low emissions; purple indicates high emissions). **b**, The points and lines show the average vulnerability scores and 95% confidence intervals for major taxonomic groups. The numbers of species are reported. The arrows show the average increase in climate vulnerability when transitioning from low- to high-emission scenarios. **c**, The points depict the proportions of at-risk species (high or critical) according to their sensitivity, exposure and adaptivity to climate change.

substantial variation across the geographic distribution of each species (average spatial coefficient of variation across species, 6%). For instance, with mitigation, the climate risk for shortfin mako sharks (*Isurus oxyrinchus*) ranges from negligible in 25% of its distribution to high or critical across 3% of its native distribution (vulnerability range, 0.11–0.8; Supplementary Fig. 40). This result highlights the importance of resolving both taxonomic and spatial aspects of climate vulnerability and risk to guide conservation. On average, species are at high or critical climate risk across 85% (s.d. = 27%) of their geographic distributions under a high-emission scenario and across 52% (s.d. = 38%) under a low-emission scenario by 2100.

Climate risk across marine ecosystems

The proportion of species at high or critical risk varies among locations, taxa and emission scenarios (Fig. 3). Ecosystems are more at risk in the tropics (30° S–30° N), in some polar regions (>60° N or S) and closer to the shore (Fig. 3a–e). A disproportionately large number (>75%) of shark, ray and mammal species are at high or critical climate risk at low latitudes (~25° N and S), with few areas escaping exposure (Fig. 3c,d). Far more species are at risk in nearshore and low-latitude ecosystems, where cumulative biodiversity peaks[28,29] (Fig. 3e). Under high emissions, 9% of the ocean contains ecosystems with at least 50% of their constituent species at high or critical climate risk, and 1% contains ecosystems where almost all (>95%) species are at high or critical risk, including some of the most biodiverse ecosystems[28,29] in the Gulf of Thailand, the Coral Triangle, northern Australia, the Red Sea, the Persian Gulf, nearshore India, the Caribbean and some Pacific islands (Fig. 3). The recurring high climate risk of nearshore ecosystems is notable, as they have also been identified as high-priority areas for biodiversity conservation and food provision[30] and are disproportionately subjected to non-climatic stressors[30,31]. Nearshore ecosystems presently support 96% of the global fishery catch yet contain the most overexploited fisheries[30]. The risk reduction achievable through emission mitigation tends to be the greatest for these regions (Fig. 3f). Under high emissions, there are very few climate refugia where many (>75%) species are at negligible climate risk (Fig. 3g). Climate refugia are mainly located in mid- and high-latitude offshore ecosystems (~40–65° N or S), predominantly in the southern hemisphere, but they are far more extensive under mitigation.

Top predators are disproportionately climate-vulnerable relative to species at lower trophic levels (TLs) (Methods), across most of the global ocean (Fig. 3h). Under high emissions, 63% of grid cells have high-TL species that are more climate-vulnerable than those lower in the food web; when considering only statistically significant effects (71% of cells), the proportion increases to 69%.

The increasing risk at higher TLs is driven by differences in life-history characteristics, size structure and metabolic costs, geographic range size and fragmentation, and exposure to human impacts and associated extinction risk of species. The variability of climate vulnerability scores among species also increases with trophic position, suggesting that in addition to creating asymmetric impacts across marine food webs, climate change may increasingly compromise their overall stability.

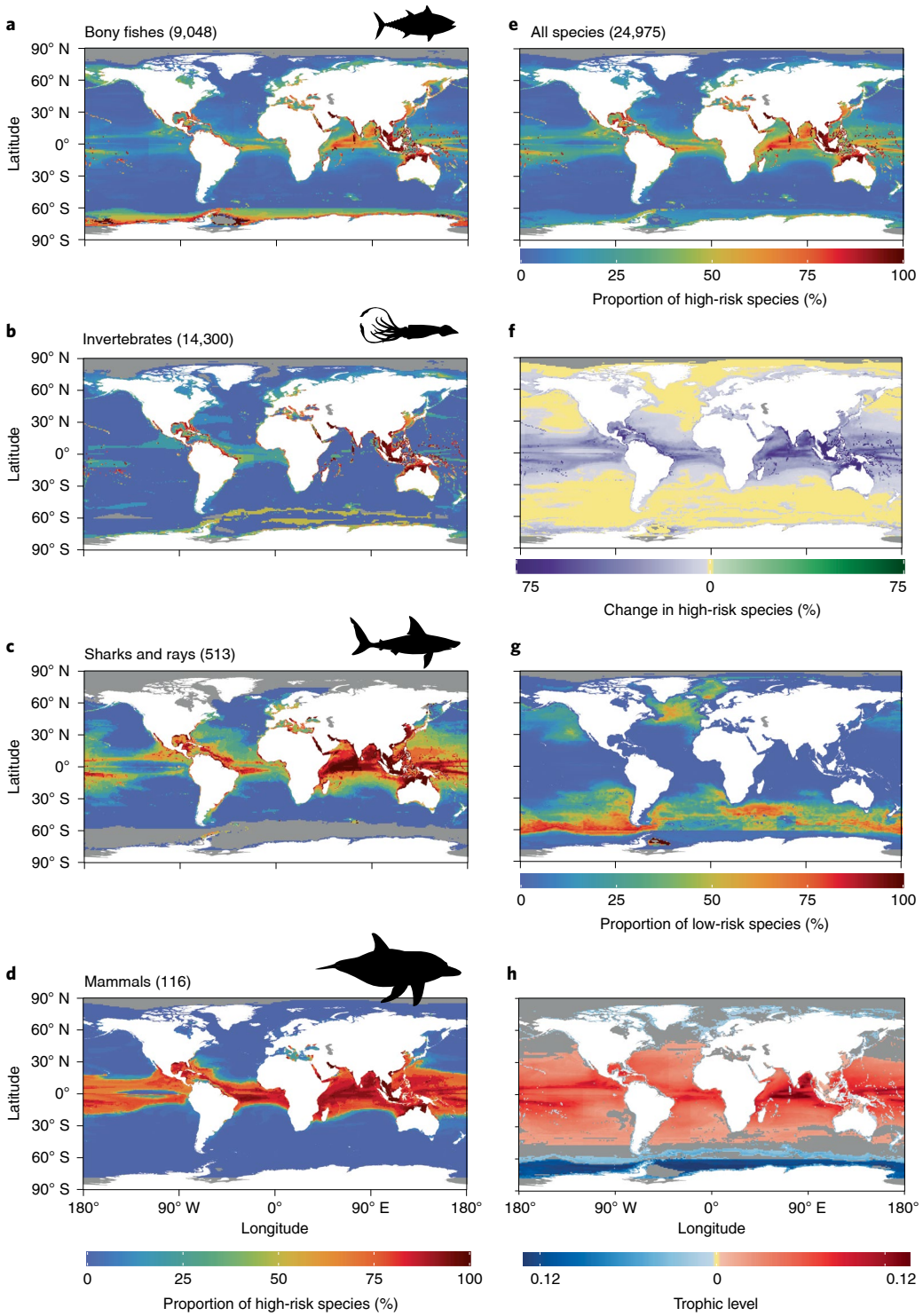

Fig. 3 | Climate risk patterns across marine ecosystems. a–e, The proportion of species at high or critical climate risk under the high-emission scenario to 2100 for bony fishes (**a**), invertebrates (**b**), sharks and rays (**c**), mammals (**d**) and all species (**e**). **f**, The change in high-climate-risk species with emission mitigation. **g**, The proportion of species at negligible climate risk under the high-emission scenario. **h**, Relationship between the TL of species and their climate vulnerability for the high-emission scenario. Red denotes areas where climate risk increases when moving up the food web. The grey shading denotes cells with insufficient data or non-significant slopes ($P > 0.05$). Basemaps in **a–h** from Natural Earth.

Cumulatively, these results suggest that climate change disproportionately affects top predators under high emissions and is likely to fundamentally alter the structure of marine ecosystems, with consequences for energy transfer, ecosystem stability and ecosystem functioning. High-TL species represent a small fraction of total biomass but include some of the most economically valuable species[32], and declines in their abundance can have drastic repercussions for ecosystems[33] and human societies. However, with substantial emission mitigation, the average global effect of TL on risk declines significantly from 0.01 to 0.008 ($P < 0.0001$), implying a

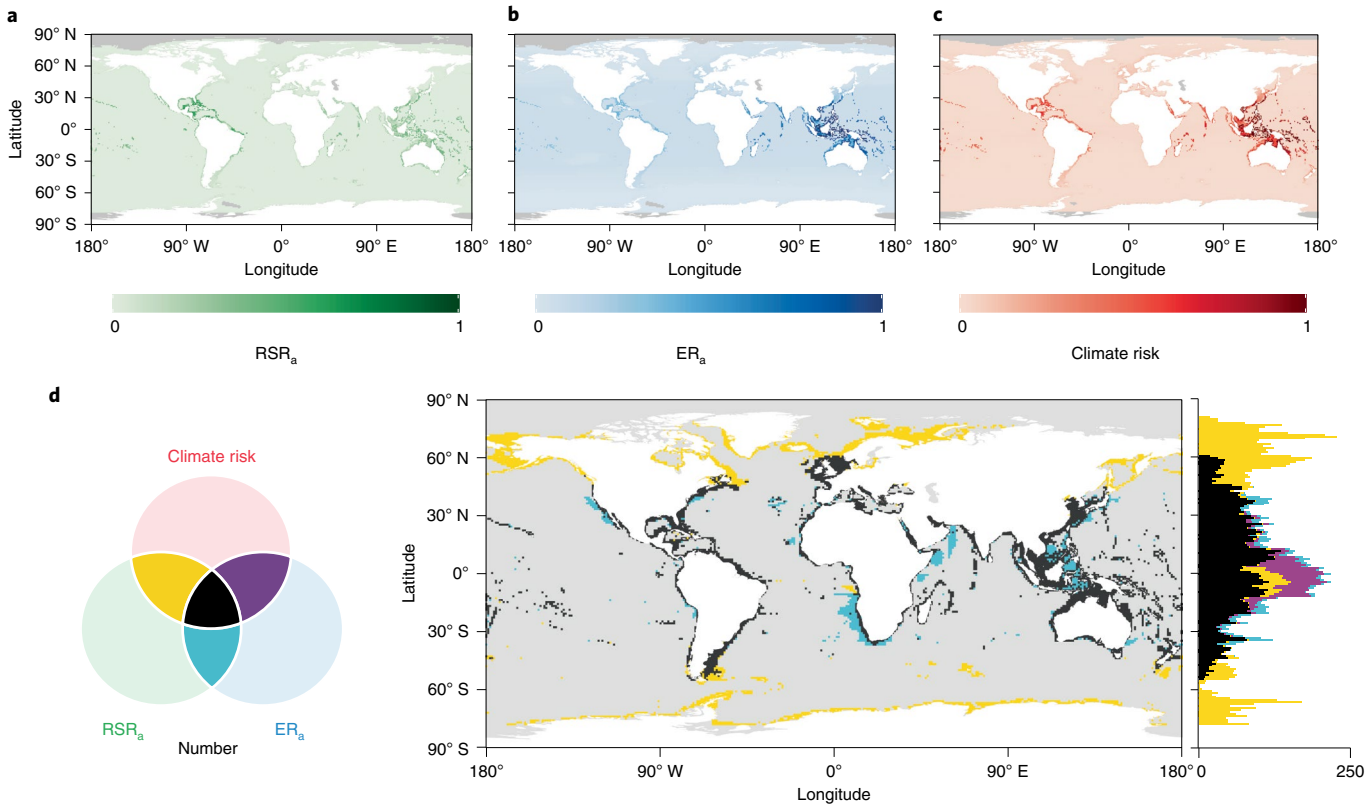

Fig. 4 | Climate risk and conservation planning. a–c, Spatial patterns in RSR$_a$ (**a**), ER$_a$ (**b**) and climate risk (**c**) in each grid cell under the high-emission scenario to 2100. **d**, Cells in which the highest RSR$_a$, ER$_a$ and climate risk intersect. The latitudinal variation is displayed on the right. Basemaps in **a–d** from Natural Earth.

reduced differential vulnerability for higher TLs. This indicates that emission mitigation reduces the likelihood of widespread ecosystem restructuring and enhances resilience to climate change relative to the high-emission scenario.

Climate risk and conservation planning

To evaluate how geographic variation in climate risk aligns with conservation priorities, we calculated three aggregate species metrics relevant to conservation planning[34–36]: aggregated range-size rarity (RSR$_a$) (Fig. 4a) to assess biodiversity and endemism[35,37], extinction risk (ER$_a$) (Fig. 4b) and climate risk (Fig. 4c). Intersecting locations with the highest RSR$_a$, ER$_a$ and climate risk identifies priority ecosystems that are in urgent need of conservation globally (Fig. 4d).

Aggregate climate risk is positively associated with RSR$_a$ and ER$_a$ under both emission scenarios (r=0.89–0.95). Under high emissions, 8% of locations have both high aggregate climate risk and RSR$_a$, while 15% have low climate risk and high RSR$_a$; 8% of species (n=610) have both high extinction (vulnerable, endangered or critically endangered) and climate risk (high or critical) scores, and 0.4% (n=28) of species are critically endangered and at critical climate risk. Globally, all three metrics intersect across 10% of the ocean; they occur across most latitudes and oceans (~70°N to S) but are primarily concentrated close to coastlines and islands, where biodiversity and endemism are elevated and where human impacts such as fishing are also higher[4].

Climate risk and socio-economic equity

We calculated the climate risk for fished species within the EEZs of 145 maritime countries and seven high-seas areas beyond national jurisdiction under both emission scenarios to 2100 (Fig. 5). With high emissions, 15% of countries (22) have >90% of all fished species at climate risk (high or critical) in their EEZs, with Asian countries projected to be disproportionately impacted (17 of 28 countries; 61%). Conversely, several countries, including many in Europe, have a lower proportion of fished species at risk, including Iceland (8%), Norway (18%) and Denmark (20%). On average, countries in Asia have the highest proportion of fished species at high or critical climate risk (86%), followed by those in North America (77%), Oceania (73%) and Africa (71%). For high-seas areas, the greatest proportions of high or critical risk species are found in the Indian (56%) and North Pacific oceans (42%), while the lowest were in the Arctic (1%) and North Atlantic (12%) oceans.

Emission mitigation resulted in fewer fished species at climate risk for all countries, but the reduction is disproportionate for many low-income countries, such as Bangladesh (−73%), Palau (−70%), Saint Vincent and the Grenadines (−70%), Micronesia (−69%) and Tanzania (−68%). Regionally, the average risk reduction is the greatest for countries in Oceania (−52%), North America (48%), Asia (41%) and South America (−35%) and the least for those in Europe (−14%).

To explore the possible impacts of climate risk on socio-economic inequalities among countries, we evaluated the relationships between the proportion of fished species at climate risk for each nation and those countries' wealth, food debt and fisheries dependence[38]. Low-income countries, which tend to have lower levels of wealth and food security and a higher dependency on fisheries, and which contribute the least to global CO_2 emissions, have systematically higher climate risks to their fisheries under the high-emission scenario (Fig. 6a–d) but also experience the greatest risk reduction through mitigation (Fig. 6e–h). Low-income countries are also subjected to many non-climatic stressors[4], probably compounding their susceptibility to climate impacts. These results are consistent with

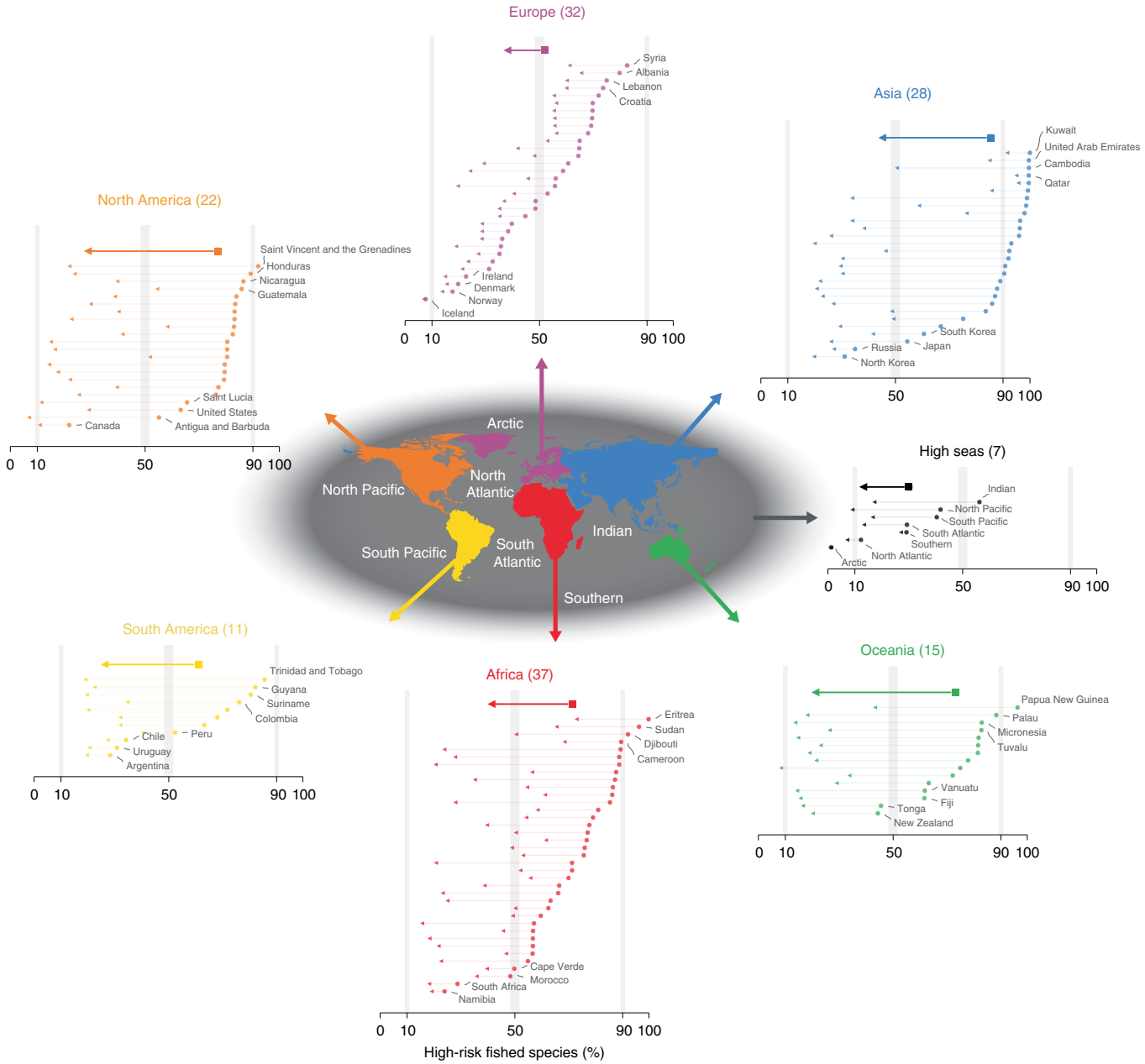

Fig. 5 | Climate risk for fisheries among maritime countries. The points and arrows indicate the proportion of fished species that are at high climate risk (high or critical) in the EEZ maritime countries (145) or high-seas ocean (7) under high and low emissions to 2100, respectively. The lines depict the magnitude of climate risk reduction with emission mitigation in all panels. The colours denote the continents or high seas. Basemap from Natural Earth.

ecosystem models that suggest low-income countries will probably experience the largest climate-driven declines in their fisheries biomass[8] and agriculture production[38] to 2100. While most low-income countries have adopted ambitious nationally determined contributions to climate mitigation[39], the excessive climate risk they face threatens to widen already substantial socio-economic equity gaps.

Caveats and future directions

Climate impacts are pervasive and complex, requiring any climate risk framework to make assumptions. First, in the absence of more comprehensive information and data, we assume that the three dimensions of risk and 12 underlying indices capture generalized climate impacts across all marine species with varying traits, habitat preferences, physiologies and life histories (for an example, see ref. [40]). Second, while our analysis follows convention[15–19] in using surface temperature as the primary measure of climate change, additional factors may alter species' responses, including changes in dissolved oxygen and pH, mixing and nutrient flux, differences in rates of warming across depths, and modified biotic interactions. While species' responses to those factors are presently less well understood, our climate risk framework represents a baseline on which to build and improve using new data and knowledge. Third, our risk metric focuses on species exposure in their existing (in situ) geographic ranges to potentially unsuitable conditions and does not account for range expansions, which represent a key aspect of species adaptivity (Supplementary Information, 'Projected loss of suitable thermal habitat'); it thus represents spatially varying risk to a species in terms of climate-driven extirpation for each part of its range. Finally, our framework depends heavily on species distribution models, which constrains the spatial resolution of

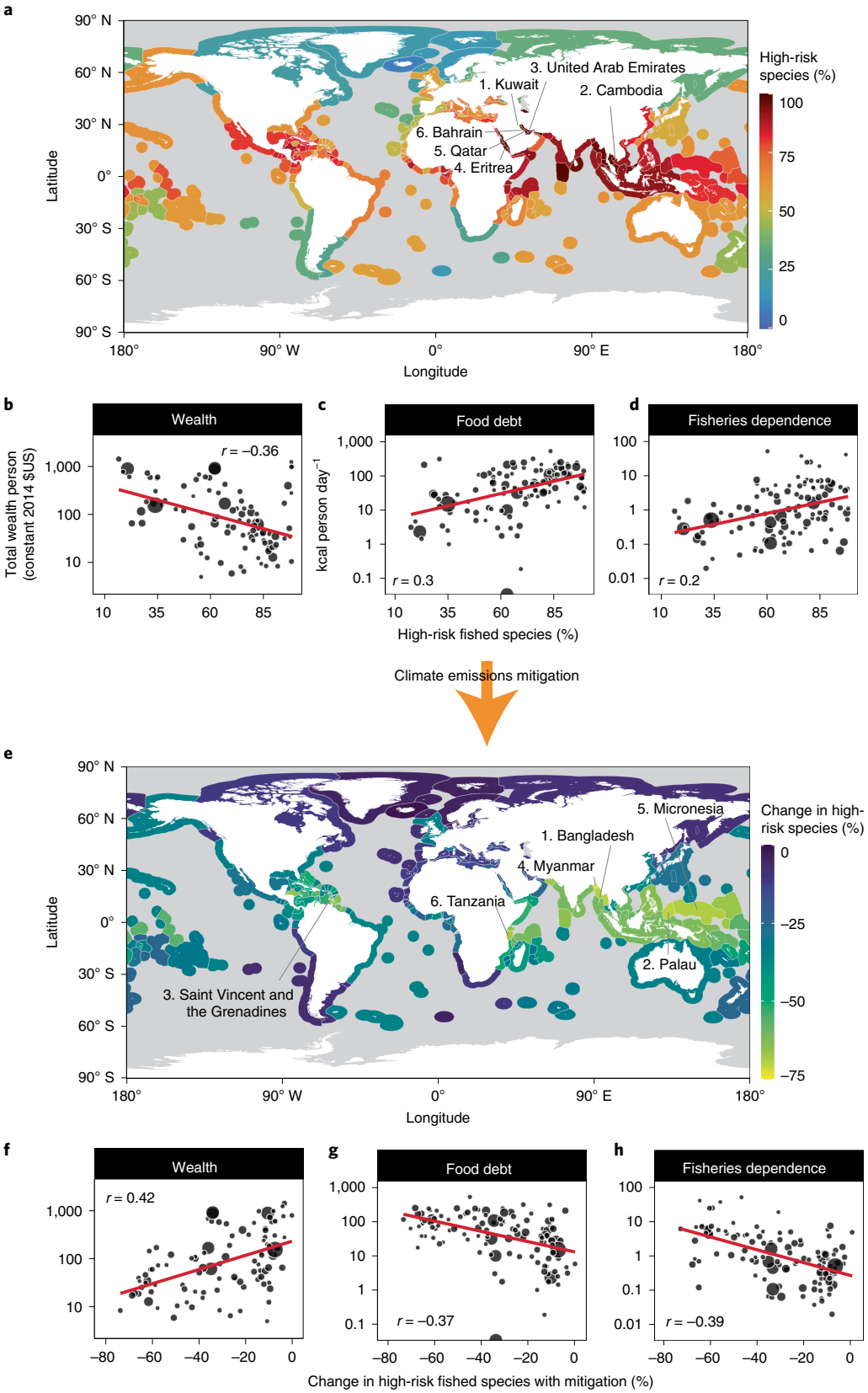

Fig. 6 | Climate risk and socio-economic equity. a, The proportion of fished species at risk (high or critical) under high emissions to 2100. **b**–**d**, Relationships between the proportion of fished species at risk for each country (**a**) and their wealth (**b**), food debt (**c**) and fishery dependence (**d**)[38]. **e**, The reduction of at-risk species in the EEZs of maritime countries. **f**–**h**, Relationships between the climate risk reduction for fished species in the EEZs of maritime countries through emission mitigation (**e**) and their wealth (**f**), food debt (**g**) and fishery dependence (**h**)[38]. In **b**–**d** and **f**–**h**, the lines are estimated from linear regressions. Basemaps in **a**,**e** from Natural Earth.

our analyses and may affect the estimation of some indices, such as geographic range extent and fragmentation; the development of higher-resolution species distribution models would alleviate this issue.

Conservation implications

Complementing the IUCN Red List of species extinction risk[27], the differential climate risk of species presented here could help prioritize conservation measures to reduce extinctions, enable adaptation and build resilience. Our analysis suggests that the climate risk for marine life varies significantly across species and within the geographic distribution of each species, emphasizing the critical importance of evaluating this risk in both ecological and geographical dimensions. In a nutshell, species' intrinsic characteristics more strongly determine their climate risk with low future emissions, but geographical variation and where species live become increasingly important under high emissions. As climate change intensifies, strategies that account for spatial variation in climate risk across individual species distributions could become increasingly critical to the continued effectiveness of conservation. In this context, the geographic patterns of ecosystem climate risk (Fig. 3) could be helpful to local, national and regional marine spatial planning, including current plans to protect at least 30% of the ocean by 2030[41]. The climate risk scores could be used to identify priority areas (Fig. 4) where minimizing interacting pressures (for example, pollution or fishing) is crucial, assess the resilience of current marine protected area coverage to climate change, or design protection networks that encompass the full range of climate risk, including hotspots and refugia[2,9,42]. Likewise, climate vulnerability and risk indicators can also support international evidence-based policy processes, such as the Convention on Biological Diversity post-2020 global biodiversity framework[41].

In addition to the global results we report, our framework can evaluate climate risk at any user-specified spatial domain resolution, using any data source to enhance its application in varied management or conservation settings. This flexibility and scalability can facilitate climate adaptation initiatives in, for instance, fisheries management[11,43] and aid in understanding the climate risk for global and transboundary fish stocks[44]. In this context, high-resolution climate layers and regionally relevant input datasets have been used to evaluate climate risk for fisheries at a regional management scale across the Northwest Atlantic Ocean[45].

Overall, our results indicate that the climate risk for marine life is strongly dependent on the magnitude of future emissions. With continued high emissions, by 2100, most species (87%) are projected to experience a high risk of adverse climate impacts and are at risk across most (85%) of their geographic distributions. Upper-TL predators are significantly more vulnerable than basal species and thus experience double-jeopardy, as they are disproportionately targeted by fisheries[46] and are associated with greater extinction risk[47]. Nearshore ecosystems that are priority areas of biodiversity conservation and food provision[30] are a concern, as they experience greater climate risk on average and multiple non-climate stressors[3,4,31].

Under high emissions, the proportion of high-risk fished species is systematically higher for low-income countries that are more dependent on fisheries[38], contribute the least to climate emissions and do the most to mitigate them[39]. Cumulatively, these results suggest that unabated emissions may hinder progress towards meeting several of the United Nations Sustainable Development Goals (SDGs) under Agenda 2030, including those aimed at reducing hunger (SDG2); improving health, well-being (SDG3) and economic inequalities (SDG10); and avoiding adverse ecosystem effects due to climate change (SDG13 and SDG14). However, under the emission mitigation scenario, the climate risk to marine life is universally less severe, with the greatest risk reduction for low-income countries. This finding emphasizes the critical importance of socio-economic development pathways for marine ecosystems' health and sustainability and supports strengthening international cooperation and financing where needed (SDG17). Our results and new assessment framework have the potential to help inform national and international initiatives to conserve biodiversity[2,48]; design, monitor and maintain protected areas[9,10]; and ensure that marine ecosystems are sustainably managed in this era of rapid climate change.

Online content

Any methods, additional references, Nature Research reporting summaries, source data, extended data, supplementary information, acknowledgements, peer review information; details of author contributions and competing interests; and statements of data and code availability are available at https://doi.org/10.1038/s41558-022-01437-y.

Received: 9 December 2021; Accepted: 30 June 2022;
Published online: 22 August 2022

References

1. Urban, M. C. Accelerating extinction risk from climate change. *Science* **348**, 571–573 (2015).
2. Brown, S. C., Wigley, T. M. L., Otto-Bliesner, B. L., Rahbek, C. & Fordham, D. A. Persistent Quaternary climate refugia are hospices for biodiversity in the Anthropocene. *Nat. Clim. Change* **10**, 244–248 (2020).
3. O'Hara, C. C., Frazier, M. & Halpern, B. S. At-risk marine biodiversity faces extensive, expanding, and intensifying human impacts. *Science* **372**, 84–87 (2021).
4. Halpern, B. S. et al. An index to assess the health and benefits of the global ocean. *Nature* **488**, 615–620 (2012).
5. Free, C. M. et al. Impacts of historical warming on marine fisheries production. *Science* **363**, 979–983 (2019).
6. Costello, C. et al. The future of food from the sea. *Nature* **588**, 95–100 (2020).
7. Lotze, H. K., Bryndum-Buchholz, A. & Boyce, D. G. in *The Impacts of Climate Change: Comprehensive Study of the Physical, Societal and Political Issues* (ed. Letcher, T.) 205–231 (Elsevier, 2021); https://doi.org/10.1016/B978-0-12-822373-4.00017-3
8. Boyce, D. G., Lotze, H. K., Tittensor, D. P., Carozza, D. A. & Worm, B. Future ocean biomass losses may widen socioeconomic equity gaps. *Nat. Commun.* **11**, 2235 (2020).
9. Tittensor, D. P. et al. Integrating climate adaptation and biodiversity conservation in the global ocean. *Sci. Adv.* **5**, 2235 (2019).
10. Wilson, K. L., Tittensor, D. P., Worm, B. & Lotze, H. K. Incorporating climate change adaptation into marine protected area planning. *Glob. Change Biol.* **26**, 3251–3267 (2020).
11. Barange, M. et al. (eds) *Impacts of Climate Change on Fisheries and Aquaculture: Synthesis of Current Knowledge, Adaptation and Mitigation Options* FAO Fisheries and Aquaculture Technical Paper No. 627 (FAO, 2018).
12. Hare, J. A. et al. A vulnerability assessment of fish and invertebrates to climate change on the northeast U.S. continental shelf. *PLoS ONE* **11**, 1–654 (2016).
13. Boyce, D. G., Fuller, S., Karbowski, C., Schleit, K. & Worm, B. Leading or lagging: how well are climate change considerations being incorporated into Canadian fisheries management? *Can. J. Fish. Aquat. Sci.* **78**, 1120–1129 (2021).
14. IPCC *Climate Change 2014: Impacts, Adaptation, and Vulnerability* (eds Field, C. B. et al.) (Cambridge Univ. Press, 2014).
15. Pacifici, M. et al. Assessing species vulnerability to climate change. *Nat. Clim. Change* **5**, 215–225 (2015).
16. de los Ríos, C., Watson, J. E. M. & Butt, N. Persistence of methodological, taxonomical, and geographical bias in assessments of species' vulnerability to climate change: a review. *Glob. Ecol. Conserv.* **15**, e00412 (2018).
17. Foden, W. B. et al. Climate change vulnerability assessment of species. *WIREs Clim. Change* **10**, e551 (2019).
18. Comte, L. & Olden, J. D. Climatic vulnerability of the world's freshwater and marine fishes. *Nat. Clim. Change* **7**, 718–722 (2017).
19. Albouy, C. et al. Global vulnerability of marine mammals to global warming. 1–12 (2020).
20. Foden, W. B. et al. Identifying the world's most climate change vulnerable species: a systematic trait-based assessment of all birds, amphibians and corals. *PLoS ONE* **8**, e65427 (2013).
21. Kesner-Reyes, K. et al. AquaMaps: algorithm and data sources for aquatic organisms. In *FishBase* v.04/2012 (eds. Froese, R. & Pauly, D.) www.fishbase.org (2016).

22. Stuart-Smith, R. D., Edgar, G. J., Barrett, N. S., Kininmonth, S. J. & Bates, A. E. Thermal biases and vulnerability to warming in the world's marine fauna. *Nature* **528**, 88–92 (2015).
23. Trisos, C. H., Merow, C. & Pigot, A. L. The projected timing of abrupt ecological disruption from climate change. *Nature* **580**, 496–501 (2020).
24. Cheung, W. W. L., Watson, R., Morato, T., Pitcher, T. J. & Pauly, D. Intrinsic vulnerability in the global fish catch. *Mar. Ecol. Prog. Ser.* **333**, 1–12 (2007).
25. IPCC *Climate Change 2021: The Physical Science Basis* (eds Masson-Delmotte, V. et al.) (Cambridge Univ. Press, in the press).
26. IPCC *Climate Change 2001: Impacts, Adaptation, and Vulnerability* (eds McCarthy, J. J. et al.) (Cambridge Univ. Press, 2001).
27. *The IUCN Red List of Threatened Species* v.2021-1 (IUCN, 2021); https://www.iucnredlist.org
28. Tittensor, D. P. et al. Global patterns and predictors of marine biodiversity across taxa. *Nature* **466**, 1098–1101 (2010).
29. Rogers, A. et al. Critical Habitats and Biodiversity: Inventory, Thresholds and Governance. *Sci. Rep.* **10**, 548 (World Resources Institute, 2020).
30. Sala, E. et al. Protecting the global ocean for biodiversity, food and climate. *Nature* **592**, 397–402 (2021).
31. Halpern, B. S. et al. Spatial and temporal changes in cumulative human impacts on the world's ocean. *Nat. Commun.* **6**, 7615 (2015).
32. Pontavice, H., Gascuel, D., Reygondeau, G., Stock, C. & Cheung, W. W. L. Climate-induced decrease in biomass flow in marine food webs may severely affect predators and ecosystem production. *Glob. Change Biol.* **27**, 2608–2622 (2021).
33. Estes, J. A., Heithaus, M., McCauley, D. J., Rasher, D. B. & Worm, B. Megafaunal impacts on structure and function of ocean ecosystems. *Annu. Rev. Environ. Res.* **41**, 83–116 (2016).
34. Jenkins, C. N., Pimm, S. L. & Joppa, L. N. Global patterns of terrestrial vertebrate diversity and conservation. *Proc. Natl Acad. Sci. USA* **110**, E2602–E2610 (2013).
35. Moilanen, A., Kujala, H. & Mikkonen, N. A practical method for evaluating spatial biodiversity offset scenarios based on spatial conservation prioritization outputs. *Methods Ecol. Evol.* **11**, 794–803 (2020).
36. Ceballos, G. & Ehrlich, P. R. Global mammal distributions, biodiversity hotspots, and conservation. *Proc. Natl Acad. Sci. USA* **103**, 19374–19379 (2006).
37. Williams, P. H., Gaston, K. J. & Humphries, C. J. Mapping biodiversity value worldwide: combining higher-taxon richness from different groups. *Proc. R. Soc. Lond. B* **264**, 141–148 (1997).
38. Blanchard, J. L. et al. Linked sustainability challenges and trade-offs among fisheries, aquaculture and agriculture. *Nat. Ecol. Evol.* **1**, 1240–1249 (2017).
39. Robiou Du Pont, Y. et al. Equitable mitigation to achieve the Paris Agreement goals. *Nat. Clim. Change* **7**, 38–43 (2017).
40. Payne, N. L. et al. Fish heating tolerance scales similarly across individual physiology and populations. *Commun. Biol.* **4**, 264 (2021).
41. *First Draft of the Post-2020 Global Biodiversity Framework* (Convention on Biological Diversity, 2021).
42. Keppel, G. et al. Refugia: identifying and understanding safe havens for biodiversity under climate change. *Glob. Ecol. Biogeogr.* **21**, 393–404 (2012).
43. Bryndum-Buchholz, A., Tittensor, D. P. & Lotze, H. K. The status of climate change adaptation in fisheries management: policy, legislation and implementation. *Fish Fish.* https://doi.org/10.1111/faf.12586 (2021).
44. Maureaud, A. et al. Are we ready to track climate-driven shifts in marine species across international boundaries? A global survey of scientific bottom trawl data. *Glob. Change Biol.* **27**, 220–236 (2021).
45. Boyce, D. G. et al. Operationalizing climate risk for fisheries in a global warming hotspot. Preprint at: https://doi.org/10.1101/2022.07.19.500650 (2022).
46. Estes, J. A. et al. Trophic downgrading of planet Earth. *Science* **333**, 301–306 (2011).
47. Olden, J. D., Hogan, Z. S. & Vander Zanden, M. J. Small fish, big fish, red fish, blue fish: size-biased extinction risk of the world's freshwater and marine fishes. *Glob. Ecol. Biogeogr.* **16**, 694–701 (2007).
48. Tittensor, D. P. et al. A mid-term analysis of progress toward international biodiversity targets. *Science* **346**, 241–244 (2014).

Methods

Identification of climate indices. The 12 climate indices, their rationales, the data sources used and supporting references are listed in Supplementary Table 1. The climate indices were selected to be grounded in ecological theory, widely accepted and validated through peer review and publication. The indices were restricted to those where the climate change impact pathways on species were generalized across them, and to maximize their unique information content and minimize redundancies; their uniqueness was evaluated by testing their collinearity ('Collinearity of climate indices' in the Supplementary Information and Extended Data Fig. 3). Parsimony was also critical to avoid pseudoreplication: indices that were easy to interpret and calculate were given priority. These various indices represent a combined approach to vulnerability assessment[17]: this approach integrates trait-based, correlative and mechanistic information and incorporates abiotic, biotic and human pressures acting across multiple biological organization levels from species to ecosystems. The 12 indices are fully described in the Supplementary Information ('Calculation of the indices') and listed in Supplementary Table 1. The climate sensitivity indices included species' thermal safety margins[18,22,49,50], vertical habitat variability and use[51–54], conservation status[55] and cumulative impacts[4,31,56–61]. The climate exposure indices were based on ensemble climate projections and included the timing of climate emergence from species' thermal niches[23,62–64], the extent of suitable thermal habitat loss[65–67], climate-related ecosystem disruption[23,68–71] and the projected climate velocity[72–74]. The adaptivity indices included the species' geographic range extent[51,72,74–78], geographic habitat fragmentation[19,79–83], maximum body length[17,19,81,84–88] and historical thermal habitat variability and use[19,89–92].

Data. All data sources are listed in Supplementary Table 2.

Taxonomic overview. Species that did not inhabit the upper 100 m of the ocean were excluded from the analyses, as were those for which the maximum depth of occurrence exceeded 1,000 m; surface temperatures could weakly define the climate risk of these species. Sensitivity analyses were used to validate these thresholds (Supplementary Fig. 41). We also excluded seabird species from the analyses, as they spend a minority of their time in surface waters. We excluded species with large freshwater distributions or that spend most of their time in freshwater habitats (for example, sturgeons, salmons, shads and eels).

The assessed species were primarily animals ($n=24{,}617$ species; 98.6%) but also included marine plants ($n=230$; 0.9%), chromists ($n=72$; 0.3%), protozoans ($n=48$; 0.2%) and bacteria ($n=8$; <0.1%) (Extended Data Fig. 1a). While marine biodiversity sampling in general is incomplete, the spatial pattern of assessed species richness herein reflects the global distribution of marine biodiversity[28], peaking at low-to-middle latitudes (0–35° N and S), along coastlines and in known hotspots (Extended Data Fig. 1b).

Native geographic distributions. Present-day native geographic distributions for marine species were predicted from AquaMaps[21] on a 0.5° global grid using environmental niche models. The models predict the probability of occurrence for each species as a function of bathymetry, upper ocean temperature, salinity, primary production and the presence of and proximity to sea ice and coasts. AquaMaps estimates have been validated using independent survey observations[93] and evaluated against alternative methodologies and independent datasets[94]. The native geographic distributions for each species were statistically rescaled to a 1° grid using bilinear interpolation to ensure that they were compatible with the input climate projections.

Thermal niches. The upper and lower thermal preferences and tolerances of marine species were obtained from the AquaMaps niche models[21]. The upper-temperature tolerance values represent the species' realized, rather than fundamental, upper thermal tolerances. To evaluate the veracity of the species' upper thermal tolerances in AquaMaps, we compared the upper thermal tolerances reported in AquaMaps against those of matching species that were available in peer-reviewed databases. In all instances, the AquaMaps realized upper thermal tolerances were positively correlated with the upper thermal tolerances in the published databases ($r=0.8$–0.88; Supplementary Fig. 2). As expected, the fundamental tolerances were generally higher than the realized tolerances in AquaMaps[50].

Maximum body lengths. The maximum body size of each species was estimated from the FishBase[95] and SeaLifeBase[96] databases. From FishBase, length–length relationships were used to calculate maximum lengths in standard units of total length. To validate the length records, the largest maximum lengths were examined to find and exclude those that are not plausible for each genus. From SeaLifeBase, the type of measurement used to assess maximum total lengths for invertebrates depended on their taxonomy. Total length was defined by the shell length and body length for gastropods, bivalves and some decapods. Total length was determined by mantle length for cephalopods, carapace length for decapods and shell height for some gastropods. The lengths (total length, mantle length, carapace length and shell height) were then compared, and the larger lengths were used to update the maximum lengths. Species with missing body length values ($n=16{,}073$) were imputed using multiple imputations by chained equations[97], a common and recognized approach for estimating diverse types of missing data[18,98]. Refer to the Supplementary Information, 'Imputation of missing data', for the complete details of the imputation procedure and sensitivity analyses.

Vertical habitat. The maximum depth of occupancy and vertical habitat range for each species were retrieved from AquaMaps[21], SeaLifeBase[96] and FishBase[95]. The maximum depth of occupancy and vertical habitat range were truncated by the maximum bathymetry present in each grid cell across each species' native geographic distribution.

Trophic position. The TLs for each species were retrieved from FishBase[95] and SeaLifeBase[96] or entered manually for 5,686 species (23%). The TLs of primary producers not available in FishBase or SeaLifeBase were set at 1, and those of zooplankton were set at 2. Grid cells where the resident species spanned <1 TL were omitted from the analysis of variation in climate vulnerability with TL.

Conservation status. The global conservation status of species was obtained from the IUCN Red List of Threatened Species[27]. The Red List places species into categories of extinction risk according to several criteria, including but not limited to their absolute population size, their trend in abundance, their metapopulation structure, the extent of occurrence and demographic factors. Red Listed species were associated with the AquaMaps[21], FishBase[95] and SeaLifeBase[96] databases using fuzzy string-matching species taxonomies (Supplementary Information, 'Fuzzy matching species traits'). Species with missing assessments or that were data deficient ($n=18{,}438$) were given a status of Least Concern. Refer to the Supplementary Information, 'Missing data', for the complete details of the analyses of missing observations, the approach to gap-filling them and the associated sensitivity analyses.

Environmental data. Per almost all climate change vulnerability analyses[15–19,99], sea surface temperature (SST) was used as the central metric of climate change; it has high spatio-temporal availability, and its effects on species are generally better understood relative to other climate variables (such as oxygen and pH). Daily SST estimates were obtained from the US National Oceanic and Atmospheric Administration 0.25° daily Optimum Interpolation Sea Surface Temperature dataset[100]. This temperature dataset has been available globally since 1981 at a spatial resolution of 4 km^2. The SST values were statistically rescaled to a global 1° grid using bilinear interpolation.

A multivariate index of cumulative human impacts on ocean ecosystems[31,59] integrates 17 global anthropogenic drivers of ecological change at a global 1 km^2 native resolution. The human impact values were statistically rescaled to a global 1° grid using bilinear interpolation.

Climate projections. An ensemble of monthly SST (°C) projections (1850–2100) was obtained from 12 published global climate models or Earth system models (ESMs) within the Coupled Model Intercomparison Project Phase 6 (CMIP6) archive (Supplementary Table 3). The models we used span a broad range of the projections of SST within the CMIP6 model set. SST projections were made under two contrasting IPCC shared socio-economic pathway (SSP) scenarios representing alternative socio-economic developments. SSP5-8.5 (fossil-fuelled development, 'taking the highway') represents continued fossil fuel development, and SSP1-2.6 (sustainability, 'taking the green road) represents an increase in sustainable development[101]. All projections were regridded onto a regular global 1° grid.

Analyses. *Design principles.* The climate risk framework incorporated several key features that are often required in applied conservation and management settings. First, it is spatially explicit. Second, it evaluates relative vulnerability on a standardized, intuitive scale and translates it into absolute risk categories. Third, it uses publicly available quantitative data that are well-validated, thus ensuring reproducibility. Fourth, it can be flexibly implemented at varying spatial scales and in different biomes and can accommodate different types of information. Fifth, it is comprehensive, evaluating all dimensions that define vulnerability and risk[14] using multiple assessment types (for example, trait-based, mechanistic and correlative)[17]. Sixth, it evaluates the statistical uncertainty (variability) associated with vulnerability. Seventh, it evaluates the impacts of projected future climate changes on species to explore mitigation measures. Finally, it operates hierarchically, maximizing its flexibility and information content (Fig. 1).

Calculation of indices. The climate indices were calculated or obtained in their native units. Each index was defined by the focal species' traits, calculated from environmental or ecological data on a geographic grid across the native geographic distribution of the focal species and/or a mix of the two, creating indices that were both taxonomically (for each species) and geographically (for each grid cell) explicit.

Standardizations ensured that the 12 climate indices were comparable on a standardized scale (range 0–1), ecologically grounded, and reproducible in future studies and over different geographic domains (for example, regional), spatial resolutions and future exposure horizons with minimal loss of information

(Supplementary Information, 'Calculation of the indices'). Reference values and scaling functions were used to meet these criteria. The reference values were selected using established guidelines such as spatial or taxonomic comparison against the global maximum[4,102]. The scaling functions described how the scaled indices varied as their unscaled analogues increased. The indices were scaled using standard approaches (for example, $\log_{10}$), by expression as a proportion of a global or theoretical maximum (for example, percentage), or using rectangular hyperbolic functions (for example, saturating hyperbola, decelerating curve and asymptotic regression). Rectangular hyperbolic functions are ubiquitous in biology[103] and have been used to describe various biological phenomena, including the reaction speed of enzymes, the nature of predator–prey interactions and ecosystem stability[103]. We use the rectangular hyperbolic function described by the exponential equation due to its wide use and ease of interpretation to standardize and normalize the climate indices (Supplementary Fig. 3). The Supplementary Information section 'Calculation of the indices' describes the equations and parameters used to normalize all 12 climate indices, while the Supplementary Information section 'Quality control and sensitivity analyses' evaluates the impacts of different standardizations on the calculation of vulnerability (Supplementary Figs. 45–47)

Spatially explicit climate vulnerability of species. Following the sensitivity analyses, our analysis was restricted to species and cells containing all 12 indices (Supplementary Fig. 42) and with less than 10% missing grid cells across their native geographic distributions (Supplementary Fig. 43). For each species within each grid cell across its geographic distribution that contained sufficient data, sensitivity, exposure and adaptivity were each calculated as the mean of the four indices that define them. The standard deviation of the vulnerability dimensions provided an estimate of their statistical uncertainty and was propagated forwards through the subsequent vulnerability calculations using inverse variance weighting as described below. Vulnerability was calculated from sensitivity, exposure and adaptivity, while statistically accounting for both the variability and the uncertainty associated with the indices of climate exposure derived from ensemble climate projections (Supplementary Information, 'Calculating climate vulnerability').

The uncertainty associated with the model-projected climate exposure of species was statistically accounted for through discounting. Discounting is common in economics and has been used to develop the ocean health index[4] to account for the greater uncertainty associated with unknown future states. Its use in the vulnerability estimation is analogous: the future exposures of species to climate change, estimated from ESM projections, are less well resolved than are their present-day sensitivities or innate adaptive capacities. Our confidence in the reliability of the projected exposure indices scales with the length of the climate projection and the number of ensemble projections. Accordingly, these factors define a discount rate ∂. Exposure indices derived from single ESMs that make longer-term climate projections are generally less reliable[8,104–106] and are thus more heavily discounted. Those derived from a larger ensemble of ESMs that make shorter-term projections are perceived as more reliable and are discounted less. The discount rate was calculated as

$$\partial = \frac{\text{Years}}{100\theta} + \frac{\text{Models}}{-25\theta} + 0.026, \tag{1}$$

where Years is the number of years in the climate projection, Models is the number of climate projections in the ensemble and θ is a scaling factor set to 40. Under this derivation, the discount rate is maximized at 5% when projections are made for ≥100 years from a single projection and is minimized at 0% when projections are made for <5 years from >19 projections. Our study evaluated climate projections from 12 models over 80 years, yielding a discount rate of 3.1%. Discounts applied to exposure are credited to present-day sensitivity, such that the maximum total adjustment is 10%, to conserve the vulnerability scaling to between zero and one. For each species within each grid cell across its geographic distribution, the discount rate was applied to the estimated exposure and sensitivity estimates as follows:

$$\breve{E}_{s,c} = [(1-\partial)(E_{s,c})], \tag{2}$$

$$\breve{S}_{s,c} = [(1+\partial)(S_{s,c})], \tag{3}$$

where $\breve{S}$ and $\breve{E}$ are the discounted sensitivity and exposure estimates for species s within cell c. Following this, the vulnerability was calculated as a weighted average of adaptivity and discounted sensitivity and exposure as

$$V_{s,c} = \frac{\left[\breve{S}_{s,c} \times \omega S_{s,c}\right]\left[\breve{E}_{s,c} \times \omega E_{s,c}\right] + [(1-\mathrm{AC}_{s,c}) \times \omega \mathrm{AC}_{s,c}]}{\omega S_{s,c} + \omega E_{s,c} + \omega \mathrm{AC}_{s,c}}, \tag{4}$$

where $V_{s,c}$ is the vulnerability and $\mathrm{AC}_{s,c}$ is the adaptivity for species s within cell c, and $\omega S_{s,c}$, $\omega E_{s,c}$ and $\omega \mathrm{AC}_{s,c}$ are the statistical reliability weights for the estimated sensitivity, exposure and adaptivity, calculated from their scaled variances. The weights for the estimated sensitivities were calculated as the inverse of their coefficients of variation:

$$\omega S_{s,c} = \left(\frac{\sigma S_{s,c}}{\mu S_{s,c}}\right)^{-1} \tag{5}$$

where

$$\mu S_{s,c} = \frac{1}{n}\sum_{i=1}^{n} S_{s,c,i} \tag{6}$$

and

$$\sigma S_{s,c} = \sqrt{\frac{\sum_{i=1}^{n}(S_{s,c,i} - \mu S_{s,c})^2}{\mathrm{NS}_{s,c}}} \tag{7}$$

where $\sigma S_{s,c}$ and $\mu S_{s,c}$ are the standard deviation and mean, respectively, of the four indices, i, that define sensitivity for species s within cell c. $\mathrm{NS}_{s,c}$ is the number of climate indices, i, that define sensitivity for species s within cell c.

Spatially inexplicit climate vulnerability of species. The vulnerability for each species (Vs) was calculated as an inverse variance-weighted mean of the vulnerabilities in each grid cell across its geographic distribution:

$$V_s = \frac{\sum_{c=1}^{n} \omega V_{s,c}\, V_{s,c}}{\sum_{c=1}^{n} \omega V_{s,c}} \tag{8}$$

while their variance-weighted standard deviations were calculated as

$$\sigma V_s = \sqrt{\frac{v_1}{v_1^2 - v_2}\sum_{c=1}^{N} \omega V_{s,c}(V_{s,c} - \mu V_{s,c})^2} \tag{9}$$

where

$$V_1 = \sum_{c=1}^{N} \omega V_{s,c} \tag{10}$$

and

$$V_2 = \sum_{c=1}^{N} \omega V_{s,c}^2 \tag{11}$$

and

$$\omega V_{s,c} = \left(\frac{\sigma V_{s,c}}{\mu V_{s,c}}\right)^{-1} \tag{12}$$

Under this derivation, greater statistical weighting is given to vulnerability estimates in grid cells where their variance (for example, the spread of the indices used to calculate them) is lower and vice versa. Species estimates will be more variable when the vulnerability is more dissimilar in the grid cells that comprise its geographic distribution and vice versa.

Climate risk for species and ecosystems. We defined climate risk thresholds to translate climate vulnerability into risk categories according to the ecological interpretation of each of the 12 climate indices (Supplementary Table 4). The risk thresholds are defined in their native units and propagated through the analysis, preserving their meaning and interpretation. This approach using thresholds is comparable to the definition of extinction risk used by the IUCN Red List of species[27] and the reasons for concern framework adopted to define climate risk by the IPCC[14,25,26]. It allows the relative vulnerability of species and communities to be translated into absolute risk categories using transparent and, where possible, empirically supported approaches[107–109]. The details of the risk thresholds used to determine climate risk for species and their justifications are listed in Supplementary Table 4.

Ecosystem patterns of climate risk. In each 1° cell, we calculated the slope (β_{TL}) of a weighted linear regression between the local vulnerability of a species and its TL. The magnitudes and directions of β_{TL} capture systematic differences between species' vulnerability given their position in the food web. The magnitude of β_{TL} quantifies how rapidly vulnerability changes when moving up one TL in the food web. The direction of β_{TL} quantifies which food web components are the most vulnerable: positive values indicate that high-TL species (such as top predators) are more vulnerable than low (such as primary producers) and vice versa. Sensitivity analyses were undertaken, omitting primary producers (TL = 1; n = 302 species) or all plankton (TL < 2.5; n = 1,095 species) or testing alternative model configurations; our results were not significantly changed by these sensitivity analyses (Supplementary Fig. 50).

Exploitation status. Exploited species were identified as those that have fisheries landings data reported in the United Nations Food and Agricultural Organization

global capture production database or the Northwest Atlantic Fisheries Organization fisheries statistics database, 2000 and 2021[110]. For each exploited species, we added all possible synonyms contained within the World Register of Marine Species taxonomic database[111].

Aggregate ecosystem indices. In each grid cell across their geographic distributions, each species' RSR was calculated as

$$\mathrm{RSR}_{s,c} = \frac{A_{s,c}}{A_s} \quad (13)$$

where $A_{s,c}$ is the surface area for species s in grid cell c, and A_s is the surface area comprising the geographic distribution of species s. Following this, RSR_a was calculated in each grid cell as the sum of RSRs for all species that live there. ER_a was calculated as the sum of the standardized IUCN Red List statuses for all species in each grid cell. Aggregate climate risk was similarly calculated as the sum of the standardized climate vulnerability scores for all species in each grid cell. Under these derivations, ecosystems where all species have low scores for extinction or climate risk or for RSR_a receive low aggregate scores, and scores increase with the number of species and their risk or RSR_a values. The aggregated scores thus account for the number of species (biodiversity) and the cumulative risk of ecosystems.

Climate risk across maritime countries. We calculated the fraction of exploited marine species that fall within different climate risk categories and that are resident within the EEZs of maritime countries under both emission scenarios. Exploited species were identified as those reported in landings databases maintained by the United Nations Food and Agricultural Organization or the Northwest Atlantic Fisheries Organization. We then evaluated the climate risk of fisheries for different countries in relation to their social and economic status indicators, including total per capita wealth (US$ per person; 1995–2014)[112], per capita food deficit (kcal per person per day; 1999–2016)[113] and fishery dependency[8].

Quality control and sensitivity analyses. Extensive sensitivity analyses were undertaken (as described in the Supplementary Information, 'Quality control and sensitivity analyses') to inform our determination of the appropriate species and data to include (Supplementary Figs. 41–45), the acceptable levels of data missingness (Supplementary Fig. 43), the impact of the standardizations on the calculations (Supplementary Figs. 44–46), the veracity of the imputations (Supplementary Fig. 47), the collinearity of the indices (Extended Data Fig. 3) and the definition of species' native geographic distributions (Supplementary Figs. 48 and 49).

Data availability

All datasets used in this paper are described and archived at the publicly available sources listed in Supplementary Table 2. Species vulnerability scores are available through the Dryad digital repository[114].

Code availability

Statistical analyses were conducted using the R statistical computing platform[115], and the code is available upon request to the corresponding author.

References

49. Pinsky, M. L., Eikeset, A. M., McCauley, D. J., Payne, J. L. & Sunday, J. M. Greater vulnerability to warming of marine versus terrestrial ectotherms. *Nature* https://doi.org/10.1038/s41586-019-1132-4 (2019).
50. Sunday, J. M., Bates, A. E. & Dulvy, N. K. Thermal tolerance and the global redistribution of animals. *Nat. Clim. Change* **2**, 686–690 (2012).
51. Laidre, K. L. et al. Quantifying the sensitivity of Arctic marine mammals to climate-induced habitat change. *Ecol. Appl.* **18**, S97–S125 (2008).
52. Rosset, V. & Oertli, B. Freshwater biodiversity under climate warming pressure: identifying the winners and losers in temperate standing waterbodies. *Biol. Conserv.* **144**, 2311–2319 (2011).
53. Peters, R. L. The greenhouse effect and nature reserves. *Biosciences* **35**, 707–717 (1985).
54. Garcia, R. A. et al. Matching species traits to projected threats and opportunities from climate change. *J. Biogeogr.* **41**, 724–735 (2014).
55. *IUCN Red List Categories and Criteria: Version 3.1* (IUCN, 2012).
56. Worm, B. et al. Impacts of biodiversity loss on ocean ecosystem services. *Science* **314**, 787–790 (2006).
57. Worm, B., Lotze, H. K., Hillebrand, H. & Sommer, U. Consumer versus resource control of species diversity and ecosystem functioning. *Nature* **417**, 848–851 (2002).
58. Worm, B. & Duffy, J. E. Biodiversity, productivity, and stability in real food webs. *Trends Ecol. Evol.* **18**, 628–632 (2003).
59. Halpern, B. S. et al. A global map of human impact on marine ecosystems. *Science* **319**, 948–952 (2008).
60. Ottersen, G., Hjermann, D. O. & Stenseth, N. C. Changes in spawning stock structure strengthen the link between climate and recruitment in a heavily fished cod (*Gadus morhua*) stock. *Fish. Oceanogr.* **15**, 230–243 (2006).
61. Le Bris, A. et al. Climate vulnerability and resilience in the most valuable North American fishery. *Proc. Natl Acad. Sci. USA* **115**, 1831–1836 (2018).
62. Henson, S. A. et al. Rapid emergence of climate change in environmental drivers of marine ecosystems. *Nat. Commun.* **8**, 14682 (2017).
63. Bates, A. E. et al. Climate resilience in marine protected areas and the 'Protection Paradox'. *Biol. Conserv.* **236**, 305–314 (2019).
64. Xu, C., Kohler, T. A., Lenton, T. M., Svenning, J.-C. & Scheffer, M. Future of the human climate niche. *Proc. Natl Acad. Sci. USA* **117**, 11350–11355 (2020).
65. Davies, T. E., Maxwell, S. M., Kaschner, K., Garilao, C. & Ban, N. C. Large marine protected areas represent biodiversity now and under climate change. *Sci. Rep.* **7**, 9569 (2017).
66. MacKenzie, B. R. et al. A cascade of warming impacts brings bluefin tuna to Greenland waters. *Glob. Change Biol.* **20**, 2484–2491 (2014).
67. Shackell, N. L., Ricard, D. & Stortini, C. Thermal habitat index of many Northwest Atlantic temperate species stays neutral under warming projected for 2030 but changes radically by 2060. *PLoS ONE* **9** (2014).
68. Boyce, D. G., Frank, K. T., Worm, B. & Leggett, W. C. Spatial patterns and predictors of trophic control across marine ecosystems. *Ecol. Lett.* **18**, 1001–1011 (2015).
69. Boyce, D. G., Frank, K. T. & Leggett, W. C. From mice to elephants: overturning the 'one size fits all' paradigm in marine plankton food chains. *Ecol. Lett.* **18**, 504–515 (2015).
70. Frank, K. T., Petrie, B., Shackell, N. L. & Choi, J. S. Reconciling differences in trophic control in mid-latitude marine ecosystems. *Ecol. Lett.* **9**, 1096–1105 (2006).
71. Frank, K. T., Petrie, B. & Shackell, N. L. The ups and downs of trophic control in continental shelf ecosystems. *Trends Ecol. Evol.* **22**, 236–242 (2007).
72. Loarie, S. R. et al. The velocity of climate change. *Nature* **462**, 1052–1056 (2009).
73. Burrows, M. T. et al. The pace of shifting climate in marine and terrestrial ecosystems. *Science* **334**, 652–655 (2011).
74. Mora, C. et al. The projected timing of climate departure from recent variability. *Nature* **502**, 183–187 (2013).
75. Poloczanska, E. S. et al. Responses of marine organisms to climate change across oceans. *Front. Mar. Sci.* **3**, 62 (2016).
76. Boyce, D. G., Lewis, M. L. & Worm, B. Global phytoplankton decline over the past century. *Nature* **466**, 591–596 (2010).
77. Burek, K. A., Gulland, F. M. D. & O'Hara, T. M. Effects of climate change on Arctic marine mammal health. *Ecol. Appl.* **18**, S126–S134 (2008).
78. Staude, I. R., Navarro, L. M. & Pereira, H. M. Range size predicts the risk of local extinction from habitat loss. *Glob. Ecol. Biogeogr.* **29**, 16–25 (2020).
79. Moore, S. E. & Huntington, H. P. Arctic marine mammals and climate change: impacts and resilience. *Ecol. Appl.* **18**, S157–S165 (2008).
80. Kaschner, K., Watson, R., Trites, A. & Pauly, D. Mapping world-wide distributions of marine mammal species using a relative environmental suitability (RES) model. *Mar. Ecol. Prog. Ser.* **316**, 285–310 (2006).
81. Gonzalez-Suarez, M., Gomez, A. & Revilla, E. Which intrinsic traits predict vulnerability to extinction depends on the actual threatening processes. *Ecosphere* **4**, 6 (2013).
82. Rogan, J. E. & Lacher, T. E. in *Reference Module in Earth Systems and Environmental Sciences* (Elsevier, 2018); https://doi.org/10.1016/B978-0-12-409548-9.10913-3
83. Warren, M. S. et al. Rapid responses of British butterflies to opposing forces of climate and habitat change. *Nature* **414**, 65–69 (2001).
84. Chessman, B. C. Identifying species at risk from climate change: traits predict the drought vulnerability of freshwater fishes. *Biol. Conserv.* **160**, 40–49 (2013).
85. Davidson, A. D. D. et al. Drivers and hotspots of extinction risk in marine mammals. *Proc. Natl Acad. Sci. USA* **109**, 3395–3400 (2012).
86. Cheung, W. W. L., Pauly, D. & Sarmiento, J. L. How to make progress in projecting climate change impacts. *ICES J. Mar. Sci.* **70**, 1069–1074 (2013).
87. Fenchel, T. Intrinsic rate of natural increase: the relationship with body size. *Oecologia* **14**, 317–326 (1974).
88. Healy, K. et al. Ecology and mode-of-life explain lifespan variation in birds and mammals. *Proc. R. Soc. B* **281**, 20140298 (2014).
89. Carilli, J., Donner, S. D. & Hartmann, A. C. Historical temperature variability affects coral response to heat stress. *PLoS ONE* **7**, e34418 (2012).
90. Guest, J. R. et al. Contrasting patterns of coral bleaching susceptibility in 2010 suggest an adaptive response to thermal stress. *PLoS ONE* **7**, e33353 (2012).
91. Donner, S. D. & Carilli, J. Resilience of Central Pacific reefs subject to frequent heat stress and human disturbance. *Sci. Rep.* **9**, 3484 (2019).
92. Rehm, E. M., Olivas, P., Stroud, J. & Feeley, K. J. Losing your edge: climate change and the conservation value of range-edge populations. *Ecol. Evol.* **5**, 4315–4326 (2015).
93. Ready, J. et al. Predicting the distributions of marine organisms at the global scale. *Ecol. Modell.* **221**, 467–478 (2010).

94. Jones, M. C., Dye, S. R., Pinnegar, J. K., Warren, R. & Cheung, W. W. L. Modelling commercial fish distributions: prediction and assessment using different approaches. *Ecol. Modell.* **225**, 133–145 (2012).
95. Froese, R. & Pauly, D. *FishBase* v.02/2022 www.fishbase.org (2022).
96. Palomares, M. L. D. & Pauly, D. *SeaLifeBase* v.11/2014 www.sealifebase.org (2022).
97. van Buuren, S. *Flexible Imputation of Missing Data* (Chapman & Hall/CRC, 2012).
98. Dahlke, F. T., Wohlrab, S., Butzin, M. & Portner, H.-O. Thermal bottlenecks in the life cycle define climate vulnerability of fish. *Science* **369**, 65–70 (2020).
99. Stortini, C. H., Shackell, N. L., Tyedmers, P. & Beazley, K. Assessing marine species vulnerability to projected warming on the Scotian Shelf, Canada. *ICES J. Mar. Sci.* **72**, 1713–1743 (2015).
100. Reynolds, R. W. et al. Daily high-resolution-blended analyses for sea surface temperature. *J. Clim.* **20**, 5473–5496 (2007).
101. Meinshausen, M. et al. The shared socio-economic pathway (SSP) greenhouse gas concentrations and their extensions to 2500. *Geosci. Model Dev.* **13**, 3571–3605 (2020).
102. Samhouri, J. F. et al. Sea sick? Setting targets to assess ocean health and ecosystem services. *Ecosphere* **3**, art41 (2012).
103. Rao, T. R. A curve for all reasons. *Resonance* **5**, 85–90 (2000).
104. Mora, C. et al. Biotic and human vulnerability to projected changes in ocean biogeochemistry over the 21st century. *PLoS Biol.* **11**, 10 (2013).
105. Lotze, H. K. et al. Ensemble projections of global ocean animal biomass with climate change. *Proc. Natl Acad. Sci. USA* https://doi.org/10.1073/pnas.1900194116 (2019).
106. Eyring, V. et al. Taking climate model evaluation to the next level. *Nat. Clim. Change* **9**, 102–110 (2019).
107. Oppenheimer, M., Little, C. M. & Cooke, R. M. Expert judgement and uncertainty quantification for climate change. *Nat. Clim. Change* **6**, 445–451 (2016).
108. Budescu, D. V., Por, H. H. & Broomell, S. B. Effective communication of uncertainty in the IPCC reports. *Climatic Change* **113**, 181–200 (2012).
109. Swart, R., Bernstein, L., Ha-Duong, M. & Petersen, A. Agreeing to disagree: uncertainty management in assessing climate change, impacts and responses by the IPCC. *Climatic Change* **92**, 1–29 (2009).
110. *NAFO Annual Fisheries Statistics Database* (NAFO, 2021).
111. Horton, T. et al. *World Register of Marine Species (WoRMS)* https://www.marinespecies.org (2020).
112. *Total Wealth per Capita, 1995 to 2014* (World Bank, 2022); https://ourworldindata.org/grapher/total-wealth-per-capita
113. *Depth of the Food Deficit in Kilocalories per Person per Day, 1992 to 2016* (World Bank, 2022); https://ourworldindata.org/grapher/depth-of-the-food-deficit
114. Boyce, D. G. et al. A climate risk index for marine life. *Dryad* https://doi.org/10.5061/dryad.7wm37pvwr (2022).
115. R Core Team R: A Language and Environment for Statistical Computing Version 4.0.4 (R Foundation for Statistical Computing, 2021).

Acknowledgements

Financial support to D.G.B. was provided by the Ocean Frontier Institute (Module G) and Oceans North. D.P.T. acknowledges support from the Jarislowsky Foundation and NSERC. S.H. acknowledges support from the National Environmental Research Council (grant no. NE/R015953/1) and from the European Union's Horizon 2020 Research and Innovation Programme under grant agreement no. 820989 (COMFORT). This research was enabled in part by support provided by ACENET (www.ace-net.ca) and Compute Canada (www.computecanada.ca).

Author contributions

D.G.B. conceived and designed the study with input from B.W., D.P.T. and N.L.S. C.G., S.H., K.K., K.K.-R., R.B.R. and P.S.-Y. provided the data. D.G.B. wrote the computer code with input from A.P. D.G.B. conducted the analyses. D.G.B., B.W. and D.P.T. drafted the manuscript. All authors reviewed the methods and edited subsequent drafts.

Competing interests

The authors declare no competing interests.

Additional information

Extended data is available for this paper at https://doi.org/10.1038/s41558-022-01437-y.

Supplementary information The online version contains supplementary material available at https://doi.org/10.1038/s41558-022-01437-y.

Correspondence and requests for materials should be addressed to Daniel G. Boyce.

Peer review information *Nature Climate Change* thanks Joseph Maina and the other, anonymous, reviewer(s) for their contribution to the peer review of this work.

Reprints and permissions information is available at www.nature.com/reprints.

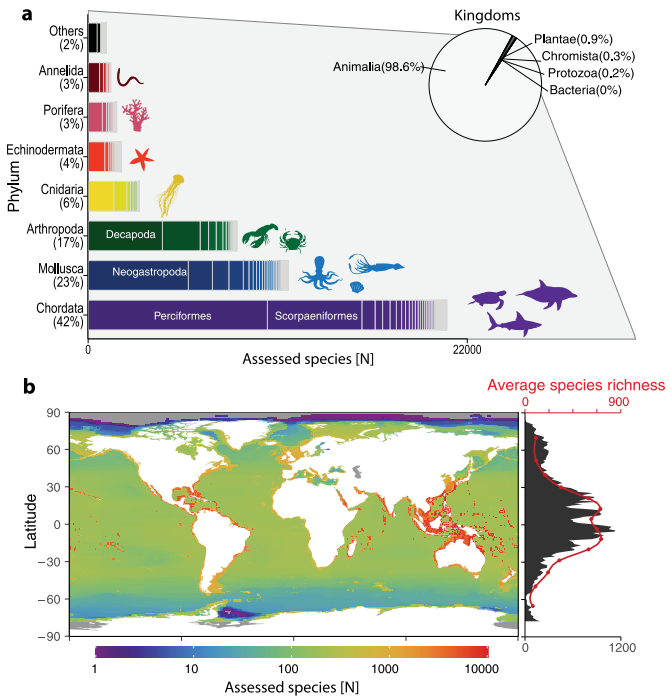

Extended Data Fig. 1 | Data availability. a) The pie chart displays the proportion of assessed species across kingdoms. Colours show the numbers of species within each animal phylum and shading within the bars shows the number of species in each taxonomic class. **b**) Spatial distribution in the number of assessed species. Colours depict the number of species assessed per 1×1° cell. The gray shaded area in the right margin shows the total number of species assessed along latitude. The red line and axis are the average species richness of all marine taxa by latitude reported in Tittensor et al.[180].

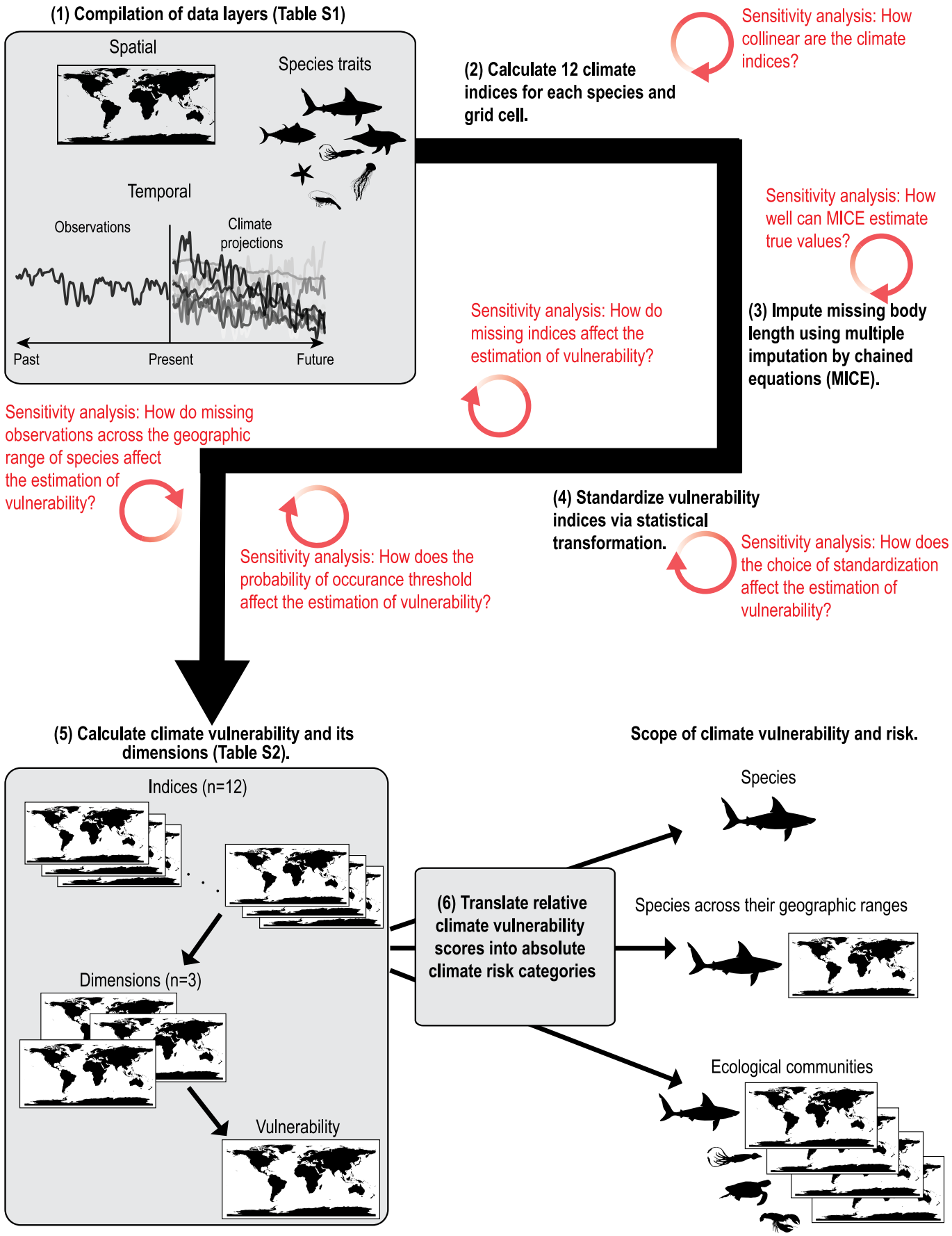

Extended Data Fig. 2 | See next page for caption.

Extended Data Fig. 2 | General overview of the steps in estimating the climate vulnerability and risk for species and ecosystems. Thick arrow and numbers denote the sequence of analyses used to estimate climate risk from the input data layers. Red depicts the sensitivity and quality-control analyses that were completed.

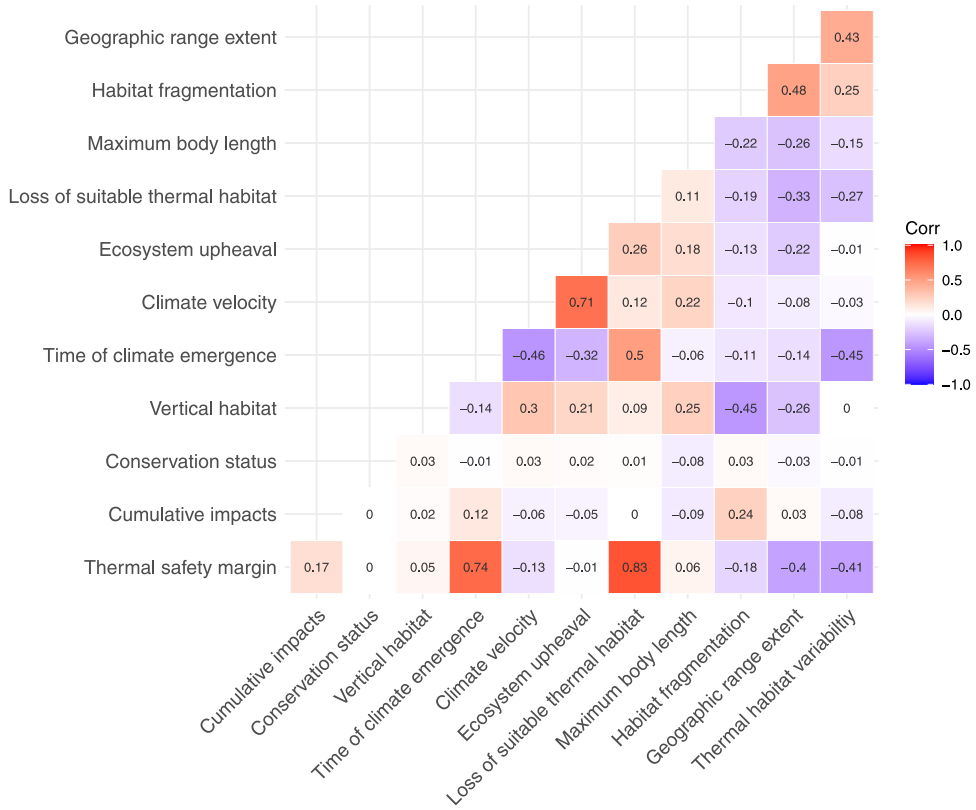

Extended Data Fig. 3 | Correlations between climate indices used to calculate climate vulnerability and risk. Colours and numbers are the correlations between climate indices calculated for each species. Colour shading and text are the direction and strength of the relationships: red are positive and blue negative correlations.